

# Sidewall Functionalization of Single-Walled Carbon Nanotubes with Nitrile Imines. Electron Transfer from the Substituent to the Carbon Nanotube

Mercedes Alvaro,<sup>†</sup> Pedro Atienzar,<sup>†</sup> Pilar de la Cruz,<sup>‡</sup> Juan L. Delgado,<sup>‡</sup> Hermenegildo Garcia,<sup>\*,†</sup> and Fernando Langa<sup>\*,‡</sup>

*Instituto de Tecnología Química CSIC-UPV, Universidad Politécnica de Valencia, 46022 Valencia, Spain, and Facultad de Ciencias del Medio Ambiente, Universidad de Castilla-La Mancha, 45071-Toledo, Spain*

Received: May 10, 2004

A new, versatile methodology for functionalization of single-walled carbon nanotubes (SWNTs), using 1,3-dipolar cycloaddition of nitrile imines to the sidewalls of SWNTs has been used to synthesize two soluble, photoactive single walled carbon nanotubes containing *n*-pentyl esters at the tips and 2,5-diarylpyrazoline units at the walls of the tubes. The success of the synthesis has been demonstrated by solution <sup>1</sup>H and <sup>19</sup>F NMR as well as UV–vis and FT-IR spectroscopy. These two compounds have been selected to have soluble single wall carbon nanotubes substituted either with an electron-poor 3,5-bis(trifluoromethyl)phenyl or electron-rich 4-(*N,N*-dimethylamino)phenyl on the C atom of the pyrazoline ring. Laser flash photolysis in dynamic flow of these carbon nanotubes in acetonitrile reveals the formation of several transient species decaying in the microsecond time scale. All the available data, including the photochemistry of model compounds, quenching experiments with electron donors and acceptors, and influence of acids, are compatible with the occurrence of an electron transfer from the electron rich substituents of the pyrazoline unit to electron acceptor termini including electron poor aryl rings and nanotube walls.

## Introduction

In recent years there has been considerable interest in the functionalization of single wall carbon nanotubes (SWNT) aimed at the control of their properties introducing the ability to respond to external stimulus.<sup>1–10</sup> In particular, light excitation could switch the semiconducting and metallic properties of the SWNT by electron or hole doping. By irradiation, a photoinduced electron transfer from or toward the nanotube walls could change in a simple and controllable way the conductivity and electronic properties of the SWNT.<sup>11,12</sup>

Functionalization of SWNT through covalent bonding can be achieved by following two different approaches in which attachment occurs predominantly either at the tube openings or at the lateral walls.<sup>13–15</sup> Though functionalization at the tips of SWNT is usually simply achieved through reaction of the terminal carboxylic groups, the strategy of sidewall functionalization still requires further development<sup>14,16</sup> and only a few procedures to graft different functional groups on the six-member aromatic rings of SWNT have been described.<sup>4,13,17</sup>

Herein, we describe a SWNT doubly functionalized at both tips with multiple alkyl chains to provide sufficient solubility of the nanotube derivative in organic solvents and lateral functionalization with diarylpyrazoline to introduce specific photochemical activity on the system. Diarylpyrazolyl units have been attached through a new procedure to functionalize SWNT consisting of the 1,3-dipolar cycloaddition of nitrile imines, a reaction that has been previously amply used for the functionalization of fullerenes.<sup>18,19</sup> Recently, theoretical studies have suggested the viability of 1,3-dipolar cycloaddition of nitrile

imine onto the sidewall of SWNT,<sup>20</sup> and formation of the pyrrolidine derivatives of SWNT through 1,3-dipolar addition has been recently reported.<sup>21</sup> Our objective is to have a soluble nanotube in which the inherent photochemical properties of unmodified SWNT could be modified due to the presence of the diarylpyrazoline chromophore. To illustrate this methodology, we have introduced in this pyrazoline moiety either a strong electron acceptor (3,5-bis(trifluoromethyl)phenyl) or an electron donor (4-(*N,N*-dimethylamino)phenyl) unit to determine the differences in the photochemical behavior arising from the lateral substitution.

## Results and Discussion

The synthesis of photoactive **2-SWNT** and **3-SWNT** was accomplished as indicated in Scheme 1. Acid purified HiPco SWNT containing carboxylic groups at the tips was reacted first with thionyl chloride, followed by addition of *n*-pentanol to obtain the ester-modified **1-SWNT**.<sup>22</sup> This ester-modified **1-SWNT** is fairly soluble in solvents such as CHCl<sub>3</sub>, CH<sub>2</sub>Cl<sub>2</sub>, THF, or acetone, and this property has been used advantageously to separate **1-SWNT** from the unreacted SWNT or insoluble products by filtration from a CHCl<sub>3</sub> suspension. Solubility of **1-SWNT** is most probably due to the shortening of the nanotube length.<sup>22</sup> In addition, solubility of the ester-modified **1-SWNT** allows one to record the <sup>1</sup>H NMR spectrum in solution. The <sup>1</sup>H NMR spectrum in CDCl<sub>3</sub> shows the expected signals corresponding to the alkoxy groups as broad peaks at about 3.80, 2.19, 1.28, and 0.89 ppm. Particularly important from the structural point of view is the signal at 3.80 ppm, indicating the ester nature of the alkyl substituents and, therefore, the covalent linking of the *n*-pentyl units to the SWNT through the carboxylic groups.

Preparation of **2-SWNT** was carried out in one pot from 3,5-bis(trifluoromethyl)benzaldehyde 4-(nitrophenyl)hydrazone<sup>23</sup> by

\* Corresponding authors. E-mail: H.G., hgarcia@qim.upv.es; F.L., flanga@amb-to.uclm.es.

<sup>†</sup> Universidad Politécnica de Valencia.

<sup>‡</sup> Universidad de Castilla-La Mancha.

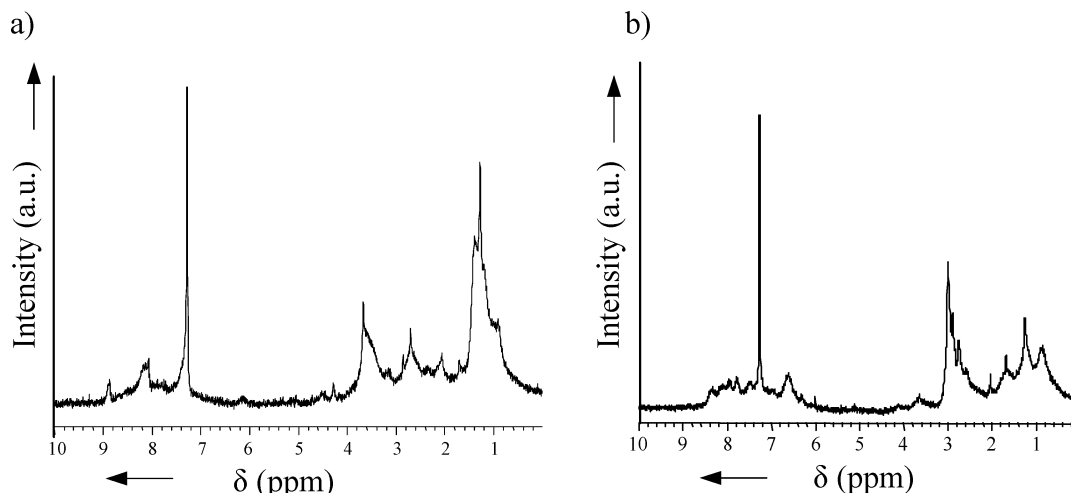
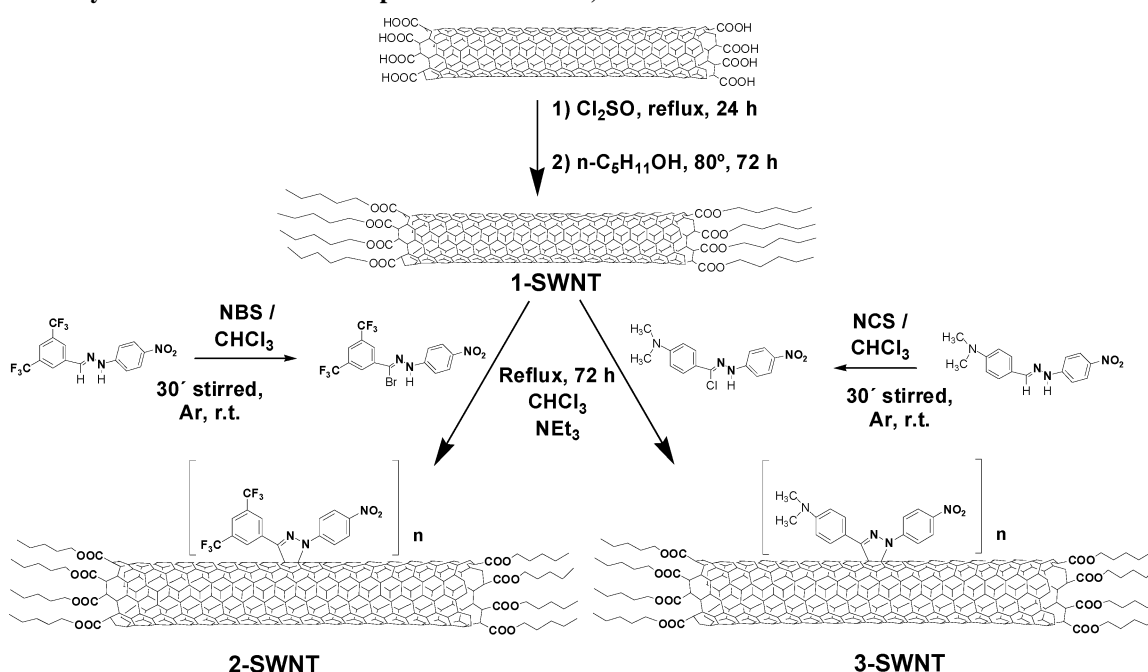


Figure 1.  $^1\text{H}$  NMR in  $\text{CDCl}_3$  of **2-SWNT** (a) and **3-SWNT** (b).

**SCHEME 1: Synthetic Route for the Preparation of Soluble, Photoactive 2-SWNT and 3-SWNT**



reaction with *N*-bromosuccinimide (NBS) in chloroform at room temperature for 30 min and subsequent addition of triethylamine to afford the nitrile imine intermediate, which is reacted in situ with the ester-modified **1-SWNT** by refluxing in chloroform for 72 h. The crude product was purified by exhaustive washings with water, diethyl ether, and pentane until disappearance of unreacted hydrazone and any other spots in TLC. The resulting **2-SWNT** was fairly soluble (without sonication) in many organic solvents including halogenated compounds, acetonitrile, DMF, and acetone and insoluble in hexane and diethyl ether. This solubility enables us to characterize **2-SWNT** by UV-vis, FT-IR, and  $^1\text{H}$  and  $^{19}\text{F}$  NMR spectroscopies.

Although the resolution of the  $^1\text{H}$  NMR was not extremely good due to the large molecular weight and the inherent inhomogeneity of carbon nanotubes, the spectrum has enough structural information to confirm definitely the chemical structure of modified nanotubes **2-SWNT**. The  $^1\text{H}$  NMR of **2-SWNT** is shown in Figure 1a. As it can be seen there, the most characteristic peaks appear as broad signals at around 8.9 and 8.2 ppm corresponding to the aromatic protons of the aryl rings having electron withdrawing substituents. In addition, the

peaks corresponding to the *n*-pentyl chains attached to the tip of the nanotubes already present in the  $^1\text{H}$  NMR spectrum of the precursor **1-SWNT** are also observed. All these features are in agreement with the structure of **2-SWNT**.

In  $^{19}\text{F}$  NMR, the presence of the characteristic peak at  $-63.11$  ppm corresponding to the trifluoromethyl groups was recorded (Figure 2a). This chemical shift is in good agreement with that of the trifluoromethyl group of the hydrazone precursor that is recorded at  $-63.35$  ppm (Figure 2b). It has to be remarked that the functionalized sample of **2-SWNT** was free from any residual hydrazone, as assessed by TLC and, therefore, the  $^{19}\text{F}$  NMR of hydrazone-free **2-SWNT** constitutes also firm evidence of the covalent attachment of the pyrazoline moiety to the nanotube.

In the UV-vis spectrum the most characteristic band appears at  $\lambda_{\text{max}}$  320 nm, which is a wavelength similar to that of 3,5-bis(trifluoromethyl)benzaldehyde 4-(nitrophenyl)hydrazone, thus confirming the presence of the diarylpyrazoline chromophore on the nanotubes (Figure 3). In contrast, the UV-vis spectrum of pristine SWNT in this region is a continuous absorption with decreasing absorptivity at longer wavelength. It was expected

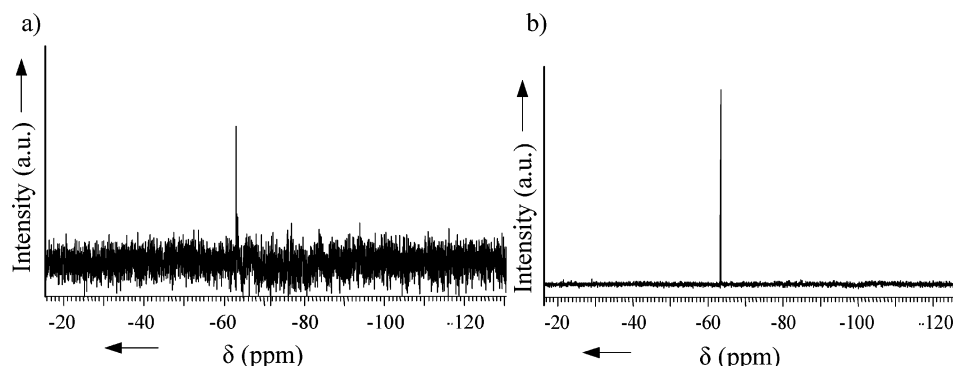


**Figure 2.**  $^{19}\text{F}$  NMR spectra in  $\text{CDCl}_3$  of **2-SWNT** (a) and 3,5-bis(trifluoromethyl)benzaldehyde 4-(nitrophenyl)hydrazone (b).

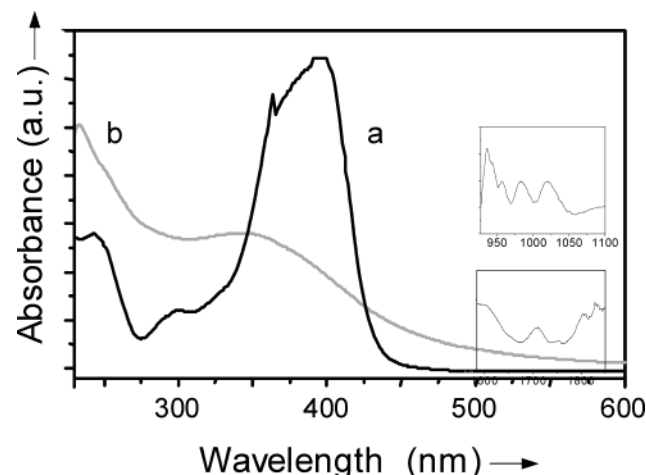


**Figure 3.** UV-vis spectrum of 3,5-bis(trifluoromethyl)benzaldehyde 4-(nitrophenyl)hydrazone (a) and **2-SWNT** (b). The insets show the van Hove singularities of **2-SWNT** recorded in the NIR region.

that irradiation at the absorption maximum of the diarylpyrazoline unit (320 nm) could lead to the initial excitation localized at the diarylpyrazoline substituent followed by sensitization of the SWNT by a mechanism of energy or electron transfer. On the other hand, the UV-NIR region of **2-SWNT** still exhibits the characteristic van Hove singularities appearing at  $\sim 1000$  and  $1800$  nm, indicating that the SWNT structure is preserved during chemical functionalization. As commented earlier for **1-SWNT**, the short tube length is also the most likely reason to explain the failure to record a TEM image of **2-SWNT**.

The FT-IR spectrum of **2-SWNT** exhibits as the most salient features the intense  $\text{C}=\text{O}$  and  $\text{NO}_2$  stretching vibrations at  $1710$  and  $1337\text{ cm}^{-1}$ , respectively, as broad bands, these wavenumbers also being in agreement with the proposed structure of the **2-SWNT** (Figure 4).

Pyrazoline-modified **2-SWNT** exhibits a characteristic emission at  $\lambda_{\text{em}} = 490$  nm upon excitation at  $400$  nm (quantum yield,  $\Phi < 0.1$ ). The corresponding spectra are shown in Figure 5. As expected, these excitation and emission spectra are very similar to those of the 3,5-bis(trifluoromethyl)benzaldehyde 4-(nitrophenyl)hydrazone precursor, indicating that these emission properties are mostly localized on the diarylpyrazoline groups of the nanotube. In related precedents in which analogous diarylpyrazoline moiety has been anchored on  $\text{C}_{60}$ , energy transfer from the pyrazoline to the  $\text{C}_{60}$  has been demonstrated by emission spectroscopy.<sup>24,25</sup> Thus, upon excitation on the pyrazoline subunit some phosphorescence emission from  $\text{C}_{60}$  has been observed accompanied by the fluorescence localized on the pyrazoline. In our case here, no evidence of energy transfer from the pyrazoline to the SWNT walls could be

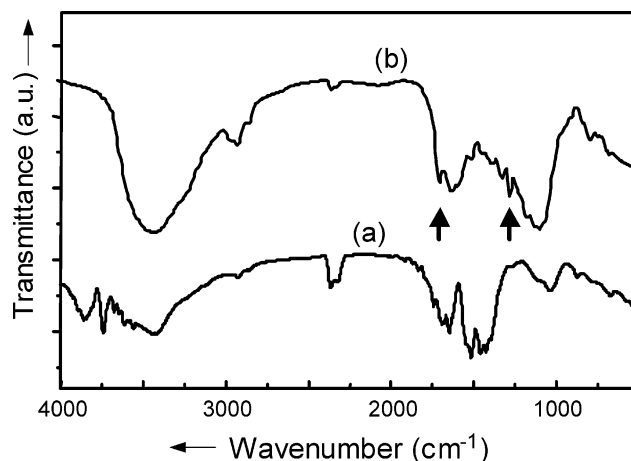


**Figure 4.** IR spectrum of a self-supported wafer of purified SWNT (a) and **2-SWNT** (b) recorded at the open air. The arrows show the presence of ester and nitro groups in **2-SWNT**.

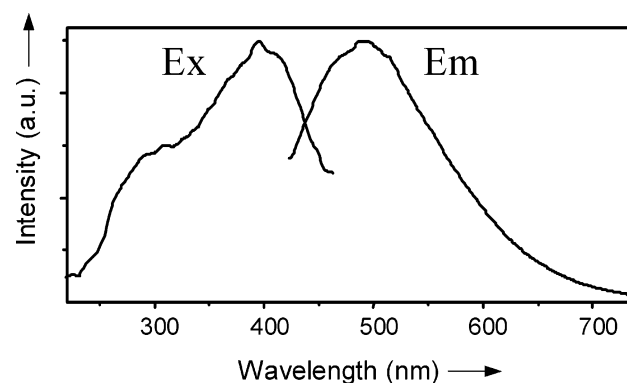


**Figure 5.** Emission (Em,  $\lambda_{\text{ex}} = 400$  nm) and excitation (Ex,  $\lambda_{\text{em}} = 490$  nm) of **2-SWNT** in  $\text{N}_2$ -purged acetonitrile recorded at room temperature.

obtained by fluorescence spectroscopy. However, this failure to observe evidence for energy transfer does not rule out its occurrence because SWNT may emit in the far-infrared region outside the wavelength range available to conventional spectrofluorometer detectors. On the other hand, we have observed previously emission from HiPco SWNT arising from localized defects of the nanotube walls having “aromatic-like substructures”, but this emission appears around the  $400$ – $500$  nm region and in our case it would be indistinguishable of the emission of the diarylpyrazoline.<sup>26</sup> Also **1-SWNT** in acetonitrile emits an intense structured photoluminescence at  $\lambda_{\text{max}}$   $315$ ,  $330$ ,  $355$ , and  $375$  nm upon excitation at  $250$ – $290$  nm.

To complete our study, we also synthesized a modified SWNT containing an electron-rich 4-(*N,N*-dimethylamino)-phenyl substituent on the C atom of the pyrazoline ring. The

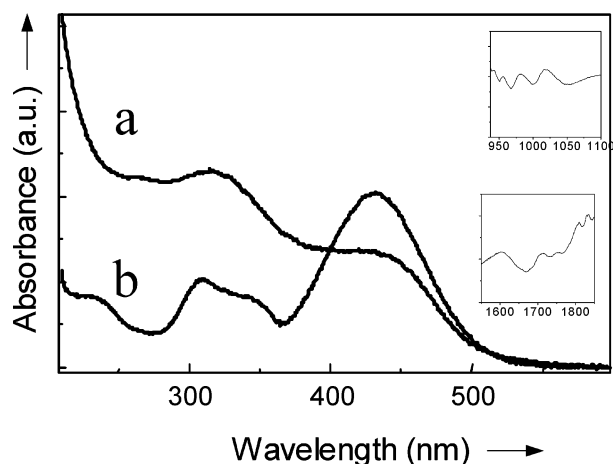


**Figure 6.** Transmission UV-vis absorption spectra in acetonitrile of **3-SWNT** (a) and 4-(*N,N*-dimethylamino)benzaldehyde 4-(nitrophenyl)hydrazone (b). The insets show the van Hove singularities of **3-SWNT** recorded in the NIR region.

synthesis of compound **3-SWNT** was accomplished following the same strategy of dipolar [3+2] cycloaddition of nitrile imine on the walls of **1-SWNT** except for the use of *N*-chlorosuccinimide (NCS) instead of NBS. Scheme 1 also illustrates the synthetic route for preparation of **3-SWNT**. Thus, dipolar cycloaddition of nitrile imines appears to be of general application for the lateral functionalization of SWNT as it is for fullerenes<sup>19,27</sup> and will indicate a chemical behavior of SWNT like that of fullerene electron-deficient aromatic rings and different from those of graphite that are rather inert. In the case of fullerenes, the curvature of the molecule and the presence of five-member rings are the main structural features responsible for their reactivity. It may be that in the case of SWNT, the structural defects play an equivalent role, facilitating dipolar cycloadditions that would be then predominantly localized close to defect sites.

**3-SWNT** was soluble in halogenated organic solvents and acetonitrile and was characterized by its <sup>1</sup>H NMR, FT-IR, UV-vis, and photoluminescence spectra. All the available spectroscopic data of **3-SWNT** are in agreement with its structure. The <sup>1</sup>H NMR spectrum of **3-SWNT** (Figure 1b) is similar to that of **2-SWNT** (vide supra) except for the presence of a broad signal centered at around 6.6 ppm, more shielded than the aromatic hydrogen atoms of **2-SWNT**, attributable to the hydrogens in ortho position respect the *N,N*-dimethylamino group.

Given the relevance for the following photochemical study, Figure 6 shows a comparison of the UV-vis absorption spectrum of **3-SWNT** and that of 4-(*N,N*-dimethylamino)benzaldehyde 4-(nitrophenyl)hydrazone.<sup>19</sup> From this figure it can be seen that **3-SWNT** exhibits in its UV-vis spectrum an absorption band characteristic of its hydrazone precursor at  $\lambda_{\text{max}}$  440 nm.

Laser flash photolysis is a powerful photochemical technique complementary to photoluminescence spectroscopy in which photogenerated transients are detected by their absorption UV-vis spectra rather than by their emission.<sup>28,29</sup> By means of laser flash photolysis even those transients that do not emit can be detected if they have characteristic absorptions in the UV-vis spectral region. Laser flash photolysis of **2-SWNT** was recorded in acetonitrile solution using as excitation source a Nd:YAG laser operating at 355 nm. This wavelength is close to that used in the above emission study. Upon consecutive irradiation of the cell with the laser (energy dose 15 mJ  $\times$  pulse<sup>-1</sup>) the sample became degraded, as evidenced by gradual

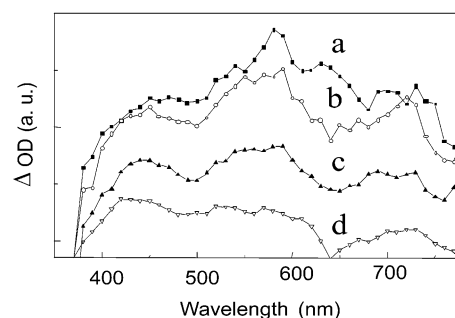


**Figure 7.** Transient spectra recorded at 30 ns (a), 50 ns (b), 100 ns (c), and 0.7  $\mu$ s (d) after laser flash photolysis (355 nm) of a  $\text{N}_2$ -purged solution of **2-SWNT** in acetonitrile under dynamic flow.

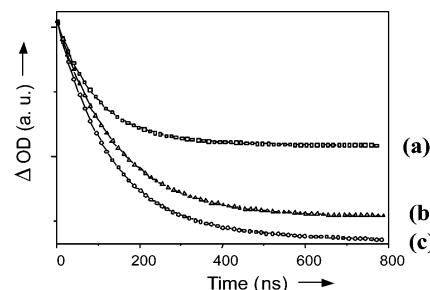


**Figure 8.** Normalized temporal profile of the signal after 355 nm excitation of a sample of  $\text{N}_2$ -purged **2-SWNT** in acetonitrile monitored at 450 (a), 580 (b), and 720 nm (c). The continuous line corresponds to the best fit of the experimental points to a three-term monoexponential decay.

variations in the consecutive transient spectra and on the steady state optical spectra after laser exposure. To ensure that the transient spectrum truly corresponds to that of the **2-SWNT**, the experiment was carried out under dynamic flow in which fresh sample is continuously exposed to the laser pulse.

The transient spectrum recorded under these conditions consists of a broad structured absorption from 400 to 800 nm and a negative absorption below 400 nm due to the intense bleaching of the ground-state absorption. Figure 7 shows the transient spectra recorded at different delay times after the laser pulse. This transient spectrum corresponds to several different species decaying in the microsecond time scale, because a comparison at the temporal profile of the signal at different wavelengths indicates that the kinetics of the signal varies depending on the region of the spectrum. Figure 8 shows the decays monitored at 450, 580, and 720 nm as well as the fitting of the experimental decays to a theoretical equation containing a series of monoexponential terms. Importantly, pristine HIPco SWNT does not exhibit any transient spectrum upon 355 nm excitation. This blank control indicates the importance of functionalization to have a photoactive SWNT.

To determine the origin and nature of these transients and considering that in related pyrazoline derivatives of  $\text{C}_{60}$  the lone electron pair of the nitrogen atom at the 1-position of the pyrazoline ring plays an important role in the photochemical process acting as electron donor,<sup>24</sup> we also recorded the laser flash photolysis transient spectrum of **2-SWNT** in the presence of Brönsted and Lewis acids such a trifluoroacetic acid and boron trichloride. As expected, addition of these acids makes the original transient spectrum recorded in their absence completely disappear, thereby pinpointing the importance of the nitrogen lone electron pair in the generation of the transient. Considering the influence of the acid in the photoprocess, a likely possibility to explain the photochemistry of **2-SWNT** compatible with the photochemistry of related  $\text{C}_{60}$  derivatives



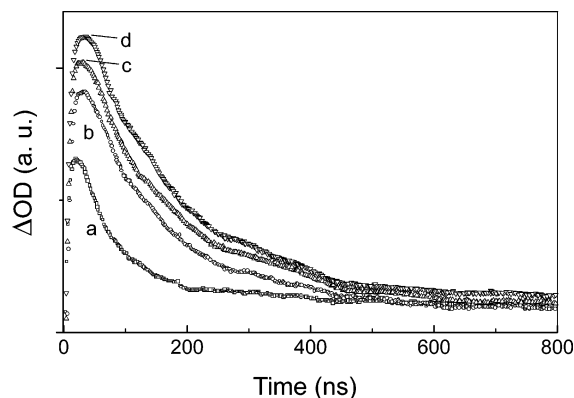


**Figure 9.** Increase of the top  $\Delta OD$  and temporal profile of the signal monitored at 600 nm recorded after 355 nm laser excitation of a  $N_2$ -purged sample of **2-SWNT** dissolved in acetonitrile (a) upon addition of an increasing concentration of  $MV^{2+}$ :  $3.3 \times 10^{-6} M$  (b);  $1 \times 10^{-5} M$  (c);  $1.6 \times 10^{-5} M$  (d). The increase in the top  $\Delta OD$  is ascribed to the formation of  $MV^{+}$  radical cation. Blank control indicates that no direct photoexcitation of  $MV^{2+}$  occurs.

would be that the transients arise from an intra- or intermolecular electron transfer from the nitrogen lone pair toward electron-acceptor moieties, the nitrophenyl and 3,5-bis(trifluoromethyl)-phenyl being obvious candidates in addition to the nanotube walls. The role of the nanotube walls as electron acceptor sites in photoinduced electron-transfer processes has been reported for the ferrocenyl<sup>30</sup> and pyrenyl<sup>31</sup> derivatives. This hypothesis is compatible with our observation of the lack of influence in the photochemistry of **2-SWNT** of typical electron donor quenchers such as triethylamine and bromide.

To support the assumption that the photoinduced electron donation occurs from the pyrazoline nitrogen atom to an acceptor, the influence of the presence of external electron acceptors such as methyl viologen ( $MV^{2+}$ ) and nitromethane was studied. The monitoring wavelength selected for this study was 600 nm, for which the  $MV^{+}$  radical cation, if formed, would absorb.<sup>32–37</sup> Blank experiments in absence **2-SWNT** demonstrate that no signal is recorded by direct excitation of  $MV^{2+}$  operating a 355 nm.

As Figure 9 shows, increasing the concentration of  $MV^{2+}$  as quencher produces an increase of the top  $\Delta OD$  of the signal at 600 nm together with an increase of the signal lifetime from 71 to 154 ns, both features indicating the photogeneration of  $MV^{+}$  radical cation.

In agreement with the behavior of the  $MV^{2+}$  quenching experiments, nitromethane also quenches the signal of **2-SWNT**, this time decreasing the amount of photogenerated transient, as illustrated in Figure 10. Nitromethane is also a good electron acceptor of the pyrazoline electron, diminishing the concentration of the photogenerated **2-SWNT** transients. The corresponding nitromethane radical anion does not exhibit any absorption at the monitored wavelength and for this reason an intensity decrease is observed in contrast to the behavior recorded for  $MV^{2+}$ .

To further confirm the assumption about the occurrence of photoinduced electron transfer, we proceeded to study the photochemical behavior as a model compound of 3,5-bis(trifluoromethyl)benzaldehyde 4-(nitrophenyl)hydrazone in acetonitrile upon 355 nm laser irradiation (Scheme 2). Only fluorescence was observed in the irradiation of the hydrazone, and no transient was detected. However, when an electron acceptor quencher such as  $C_{60}$  was added to the solution, then a transient spectrum similar to that shown in Figure 6 was recorded. In this case, [60]fullerene would be a quencher comparable to

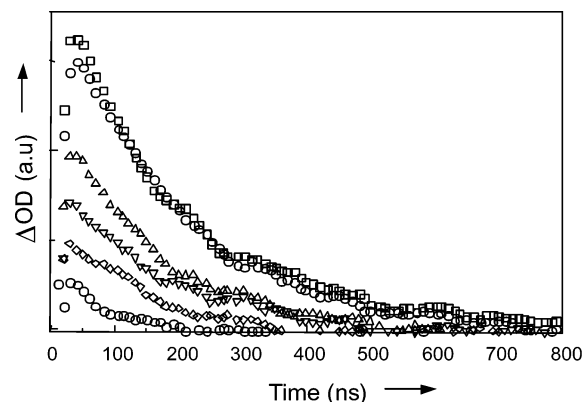


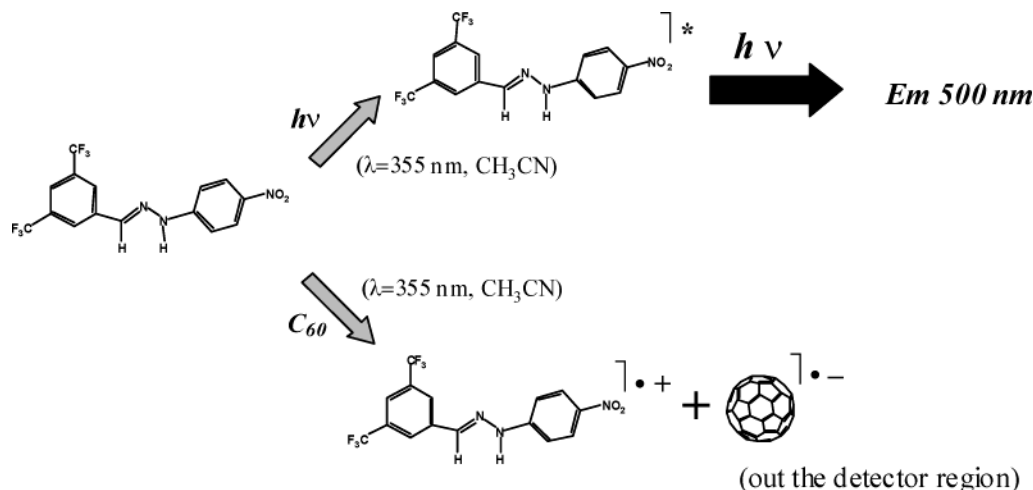
**Figure 10.** Temporal profile of the signal monitored at 600 nm after 355 nm excitation of a  $N_2$ -purged sample of **2-SWNT** in acetonitrile solution recorded upon addition of increasing concentrations of nitromethane: 0 M ( $\square$ );  $6.15 \times 10^{-5} M$  ( $\bullet$ );  $1.23 \times 10^{-4} M$  ( $\Delta$ );  $1.84 \times 10^{-4} M$  ( $\nabla$ );  $2.46 \times 10^{-4} M$  ( $\diamond$ );  $3.08 \times 10^{-4} M$  ( $\circ$ ).

SWNT. This observation lends some support to the proposed interaction between the nanotube walls and the pyrazoline units in **2-SWNT**. Therefore, the behavior of model hydrazone is in agreement with the proposal of localized excitation and with the occurrence of a photoinduced electron transfer upon light absorption on the pyrazoline moiety.

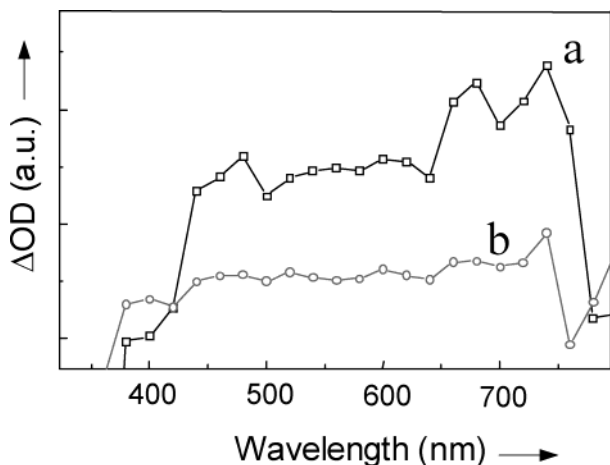
Modified nanotube **3-SWNT** was also submitted to laser flash photolysis under the dynamic flow and the same conditions, whereby a transient spectrum somewhat different from that of **2-SWNT** was recorded. Besides ground-state bleaching appearing as negative absorption at wavelengths below 400 nm and the structured continuous absorption also present in **2-SWNT**, the most characteristic spectroscopic feature is an intense absorption at 720 nm with a shoulder at 670 nm, which is attributable to the radical cation localized in the *p*-(*N,N*-dimethylamino)-phenyl substructure of **3-SWNT**. In this case, as could be anticipated, the *p*-(*N,N*-dimethylamino)phenyl group would act as an electron donor substituent upon photoexcitation. Figure 11 shows the transient spectra recorded for **3-SWNT** at two different time delays after the laser pulse.

A rationalization of the photochemistry observed for **2-SWNT** and **3-SWNT** is provided in Scheme 3 in which the possible sites for electron transfer and emission around the pyrazoline substitution have been indicated.

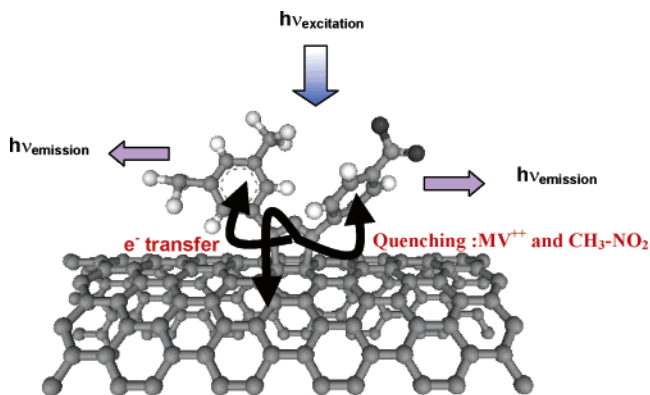
In summary, 1,3-dipolar cycloaddition of nitrile imines, prepared in situ from hydrazones, appears as a simple, versatile and general procedure to functionalize SWNTs, this finding making alike the chemistry of fullerenes and SWNTs. By appropriate functionalization at the tips and walls of SWNT, samples of modified SWNT have been prepared that, being soluble in organic solvents, contain photoactive diarylpyrazoline units covalently attached to the walls. Emission spectroscopy of **2-SWNT** and **3-SWNT** shows that the emission is mainly localized on the diarylpyrazoline substructure but, on the other hand, laser flash photolysis demonstrates the photogeneration of transients different from the model compounds showing the interaction of the diarylpyrazoline and the nanotube. Quenching experiments support the electron migration from the pyrazoline nitrogen lone pair or from the electron-rich 4-(*N,N*-dimethylamino)phenyl substituent to electron acceptor subunits of the modified SWNT. Further studies are directed to synthesize modified SWNT with the optimum efficiency of long-lived charge separation to demonstrate their applicability to the photochemical control of the properties and in photovoltaic cells.<sup>38,39</sup>

**SCHEME 2: Proposal for the Photoprocesses after 355 nm Laser Excitation of 3,5-Bis(trifluoromethyl)benzaldehyde 4-(Nitrophenyl)hydrazone and Adding C<sub>60</sub>**


Similar transient spectrum as **2-SWNT**



**Figure 11.** Transient spectra recorded at 0.2  $\mu$ s (a) and 0.8  $\mu$ s (b) after laser flash photolysis (355 nm) of a N<sub>2</sub>-purged solution of 3-SWNT in acetonitrile under dynamic flow.

**SCHEME 3: Pictorial Illustration of the Photoprocesses Occurring on 2-SWNT upon Excitation that Are Compatible with the Experimental Observation**

**Experimental Section**

**General Information.** <sup>1</sup>H NMR and <sup>19</sup>F NMR spectra were recorded in CDCl<sub>3</sub> as solvent on a Varian 200 apparatus. UV-vis absorption spectra were obtained in acetonitrile using quartz cuvettes on a Shimadzu spectrophotometer. FT-IR spectra were recorded on a Nicolet Impact 410 spectrophotometer using

KBr disks or self-supported wafers (**2-SWNT**) compressed to 2 Ton  $\times$  cm<sup>-2</sup> for 2 min. Photoluminescence measurements were performed in acetonitrile solution at room temperature in N<sub>2</sub>-purged septum-capped quartz cells in an Edinburgh FL3000 spectrofluorometer using a Xe-doped mercury lamp and a Czerny-Turner monochromator. Laser flash photolysis experiments were carried out using the third (355 nm) harmonic of a Q-switched Nd:YAG laser (Spectron Laser Systems, UK; pulse width ca. 9 ns and 35 mJ  $\times$  pulse<sup>-1</sup>). The signal from the monochromator/photomultiplier detection system was captured by a Tektronix TDS640A digitizer and transferred to a PC computer that controlled the experiment and provided suitable processing and data storage capabilities. Fundamentals and details of similar time-resolved laser setup have been published elsewhere.<sup>40</sup>

**Preparation of Ester-Modified 1-SWNT.** A purified HiPco SWNT sample (Carboxlex 50 mg) was treated with a concentrated HCl solution to recover all the carboxylic acid groups in the nanotube, followed by refluxing in thionyl chloride (2 mL) for 24 h to convert the carboxylic acids into acyl chlorides. Thionyl chloride was removed by washing with anhydrous THF, and the solvent was evacuated under reduced pressure. Then the acyl chloride nanotube was mixed in a flask with 2 g of *n*-pentanol, and the resulting solution was heated to 80 °C and stirred for 72 h under argon. The excess of *n*-pentanol was removed by vacuum distillation. The residue was extracted several times with chloroform to obtain a dark brown solution that was filtered (Swinney Millipore 0.2  $\mu$ m filter) to ensure separation from nonsoluble SWNT. The solvent was removed on a rotary evaporator yielding the ester-modified **1-SWNT** (22 mg). <sup>1</sup>H NMR (CDCl<sub>3</sub>):  $\delta$  3.80 (bs), 2.19 (bs), 1.28 (bs), 0.89 (bs). UV-vis (CH<sub>2</sub>Cl<sub>2</sub>):  $\lambda_{\text{max}}$ /nm 229.

**Preparation of 2-SWNT.** A solution of 3,5-bis(trifluoromethyl)benzaldehyde 4-(nitrophenyl)hydrazone (1 g, 2.65 mmol) and NBS (0.47 g, 2.65 mmol) in chloroform was stirred for 30 min at room temperature under argon. Triethylamine (0.53 g, 5.3 mmol) and **1-SWNT** (30 mg) were then added, and the resulting solution was heated at reflux temperature under argon for 72 h. The crude product was purified by washing with water, the organic phase was evaporated on a rotary evaporator, and the solid was purified by redispersing and centrifuging several times with fresh aliquots (2 mL) of diethyl ether and pentane. <sup>1</sup>H NMR (CDCl<sub>3</sub>):  $\delta$  8.89 (bs), 8.16 (bs), 3.61 (bs), 2.70 (bs),

2.05 (bs), 1.38 (bs), 0.90 (bs).  $^{19}\text{F}$  NMR ( $\text{CDCl}_3$ ):  $\delta$  -63.11. UV-vis ( $\text{CH}_2\text{Cl}_2$ ):  $\lambda_{\text{max}}$ /nm 233, 346. FT-IR (ATR): 2923, 1710, 1337  $\text{cm}^{-1}$ .

**Preparation of 3-SWNT.** A solution of 4-(*N,N*-dimethylamino)benzaldehyde 4-(nitrophenyl)hydrazone (1 g, 3.16 mmol) and dry pyridine (20  $\mu\text{L}$ ) in dry chloroform was cooled to 0  $^\circ\text{C}$  under argon. Then, 0.42 g (3.16 mmol) of NCS was added, and the mixture was stirred for 30 min. After addition of 1-SWNT (30 mg) and triethylamine (0.53 g, 5.3 mmol), the solution was stirred at room temperature under argon for 72 h. The crude product was purified by washing with water, the organic phase was evaporated on a rotary evaporator, and the solid was purified by redispersing and centrifuging several times with fresh aliquots (2 mL) of diethyl ether and pentane.  $^1\text{H}$  NMR ( $\text{CDCl}_3$ ):  $\delta$  7.40–8.40 (bs), 6.41–6.76 (bs), 3.66 (bs), 2.56–3.00 (bs), 2.25 (bs), 1.86 (bs), 0.90 (bs). UV-vis ( $\text{CH}_2\text{Cl}_2$ ):  $\lambda_{\text{max}}$ /nm 229, 272, 320, 430. FT-IR (ATR): 2958, 1720, 1610, 1480  $\text{cm}^{-1}$ .

**Acknowledgment.** Financial support by the DGES (projects MAT2003-1226 and BQU2001-1512), the Junta de Comunidades de Castilla-La Mancha (F.L., project PAI-02-023) and Generalidad Valenciana (H.G., grupos 03-020) is gratefully acknowledged. P.A. thanks the Spanish Ministry of Science and Technology for a postgraduate scholarship.

## References and Notes

- Qu, L.; Martin, R. B.; Huang, W.; Fu, K.; Zweifel, D.; Lin, Y.; Sun, Y.-P.; Bunker, C. E.; Harruff, B. A.; Gord, J. R.; Allard, L. F. *J. Chem. Phys.* **2002**, *117*, 8089.
- Peng, H.; Reverdy, P.; Khabashesku, V. N.; Margrave, J. L. *Chem. Commun.* **2003**, 362.
- Khabashesku, V. N.; Billups, W. E.; Margrave, J. L. *Acc. Chem. Res.* **2002**, *35*, 1087.
- Georgakilas, V.; Voulgaris, D.; Vazquez, E.; Prato, M.; Guldi, D. M.; Kukovecz, A.; Kuzmany, H. *J. Am. Chem. Soc.* **2002**, *124*, 14318.
- Haremza, J. M.; Hahn, M. A.; Krauss, T. D.; Chen, S.; Calcines, J. *Nano Lett.* **2002**, *2*, 1253.
- Azamian, B. R.; Coleman, K. S.; Davis, J. J.; Hanson, N.; Green, M. L. H. *Chem. Commun.* **2002**, 366.
- Shim, M.; Javey, A.; Kam, N. W. S.; Dai, H. *J. Am. Chem. Soc.* **2001**, *123*, 11512.
- Saini, R. K.; Chiang, I. W.; Peng, H.; Smalley, R. E.; Billups, W. E.; Hauge, R. H.; Margrave, J. L. *J. Am. Chem. Soc.* **2003**, *125*, 3617.
- Diehl, M. R.; Steuerman, D. W.; Tseng, H.-r.; Vignon, S. A.; Star, A.; Celestre, P. C.; Stoddart, J. F.; Heath, J. R. *ChemPhysChem* **2003**, *4*, 1335.
- Strano, M. S.; Dyke, C. A.; Usrey, M. L.; Barone, P. W.; Allen, M. J.; Shan, H.; Kittrell, C.; Hauge, R. H.; Tour, J. M.; Smalley, R. E. *Science* **2003**, *301*, 1519.
- Kymakis, E.; Alexandrou, I.; Amaratunga, G. A. J. *J. Appl. Phys.* **2003**, *93*, 1764.
- Kymakis, E.; Amaratunga, G. A. J. *J. Appl. Phys. Lett.* **2002**, *80*, 112.
- Hirsch, A. *Angew. Chem., Int. Ed.* **2002**, *41*, 1853.
- Bahr, J. L.; Tour, J. M. *J. Mater. Chem.* **2002**, *12*, 1952.
- Georgakilas, V.; Kordatos, K.; Prato, M.; Guldi, D. M.; Holzinger, M.; Hirsch, A. *J. Am. Chem. Soc.* **2002**, *124*, 760.
- Banerjee, S.; Kahn, M. G. C.; Wong, S. S. *Chem. Eur. J.* **2003**, *9*, 1898.
- Tagmatarchis, N.; Georgakilas, V.; Prato, M.; Shinohara, H. *Chem. Commun.* **2002**, 2010.
- Langa, F.; de la Cruz, P.; Espildora, E.; de la Hoz, A.; Bourdelande, J. L.; Sanchez, L.; Martin, N. *J. Org. Chem.* **2002**, *66*, 5033.
- Espildora, E.; Delgado, J. L.; de la Cruz, P.; de la Hoz, A.; Lopez-Arza, V.; Langa, F. *Tetrahedron* **2002**, *58*, 5821.
- Lu, X.; Tian, F.; Xu, X.; Wang, N.; Zhang, Q. *J. Am. Chem. Soc.* **2003**, *125*, 10459.
- Tasis, D.; Tagmatarchis, N.; Georgakilas, V.; Prato, M. *Chem. Eur. J.* **2003**, *9*, 4000.
- Alvaro, M.; Atienzar, P.; de la Cruz, P.; Delgado, J. L.; Garcia, H.; Langa, F. *Chem. Phys. Lett.* **2004**, *386*, 342.
- Delgado, J. L.; de la Cruz, P.; López-Arza, V.; Langa, F. *Tetrahedron* **2004**, *45*, 1651.
- Ammaroli, N.; Accorsi, G.; Gisselbrecht, J.-P.; Gross, M.; Krasnikov, V.; Tsamouras, D.; Hadziioannou, G.; Gomez-Escalonilla, M. J.; Langa, F.; Eckert, J.-F.; Nierengarten, J.-F. *J. Mater. Chem.* **2002**, *12*, 2077.
- Matsubara, Y.; Tada, H.; Nagase, S.; Yoshida, Z.-i. *J. Org. Chem.* **1995**, *60*, 5372.
- Alvaro, M.; Atienzar, P.; Bourdelande, J. L.; Garcia, H. *Chem. Commun.* **2002**, 3004.
- Yurovskaya, M. A.; Ovcharenko, A. A. *Chem. Heterocycl. Comput.* **1998**, *34*, 261.
- Wilkinson, F.; Kelly, G. Diffuse Reflectance Flash Photolysis. In *Handbook of Organic Photochemistry*; Scaiano, J. C., Ed.; CRC Press: Boca Raton, FL, 1989; Vol. 1, p 293.
- Bohne, C.; Redmond, R. W.; Scaiano, J. C. Use of the Photophysical Techniques in the Study of Organized Assemblies. In *Photochemistry in Organized and Constrained Media*; Ramamurthy, V., Ed.; VCH: New York, 1991; Chapter 3.
- Guldi, D. M.; Marcaccio, M.; Paolucci, D.; Paolucci, F.; Tagmatarchis, N.; Tasis, D.; Vazquez, E.; Prato, M. *Angew. Chem., Int. Ed.* **2003**, *42*, 4206.
- Alvaro, M.; Atienzar, P.; Bourdelande, J. L.; Garcia, H. *Chem. Phys. Lett.* **2004**, *384*, 119.
- Kasuga, K.; Hayashi, H.; Handa, M. *Chem. Lett.* **1991**, 1877.
- Braterman, P. S.; Song, J. I. *J. Org. Chem.* **1991**, *56*, 4678.
- Feng, Q.; Yue, W.; Cotton, T. M. *J. Phys. Chem.* **1990**, *94*, 2082.
- Shiraishi, H.; Buxton, G. V.; Wood, N. D. *Radiat. Phys. Chem.* **1989**, *33*, 519.
- Stargardt, J. F.; Hawkrige, F. M. *Anal. Chim. Acta* **1983**, *146*, 1.
- Solar, S.; Solar, W.; Getoff, N.; Holcman, J.; Sehested, K. *J. Chem. Soc., Faraday Trans.* **1982**, *78*, 2467.
- Wu, W.; Zhang, S.; Li, Y.; Li, J.; Liu, L.; Qin, Y.; Guo, Z.-X.; Dai, L.; Ye, C.; Zhu, D. *Macromolecules* **2003**, *36*, 6286.
- Kymakis, E.; Amaratunga, G. A. J. *J. Appl. Phys. Lett.* **2002**, *80*, 112.
- Hadel, L. M. Laser Flash Photolysis. In *Handbook of Organic Photochemistry*; Scaiano, J. C., Ed.; CRC Press: Boca Raton, FL, 1989.